

Published in final edited form as:

Biol Psychiatry. 2011 June 1; 69(11): 1043–1051. doi:10.1016/j.biopsych.2011.02.013.

Type 1 Equilibrative Nucleoside Transporter Regulates Ethanol Drinking through Accumbal *N*-Methyl-D-Aspartate Receptor Signaling

Hyung Wook Nam¹, Moonnoh R. Lee¹, Yu Zhu^{1,5}, Jinhua Wu¹, David J. Hinton¹, Sun Choi¹, Taehyun Kim¹, Nora Hammack¹, Jerry C.P. Yin⁴, and Doo-Sup Choi^{1,2,3}

¹Department of Molecular Pharmacology and Experimental Therapeutics, Mayo Clinic College of Medicine, Rochester, Minnesota 55905

²Department of Psychiatry and Psychology, Mayo Clinic College of Medicine, Rochester, Minnesota 55905

³Molecular Neuroscience Program, Mayo Clinic College of Medicine, Rochester, Minnesota 55905

⁴Department of Genetics and Neurology, University of Wisconsin, Madison, Wisconsin 53706

Abstract

Background—Mice lacking type 1 equilibrative nucleoside transporter (*ENT1*^{-/-}) exhibit increased ethanol-preferring behavior compared to wild-type littermates. This phenotype of *ENT1*^{-/-} mice appears to be correlated with increased glutamate levels in the nucleus accumbens (NAc). However, little is known about the downstream consequences of increased glutamate signaling in the NAc.

Methods—To investigate the significance of the deletion of *ENT1* and its effect on glutamate signaling in the NAc, we employed microdialysis and iTRAQ proteomics. We validated altered proteins using Western blot analysis. We then examined the pharmacological effects of the inhibition of the *N*-Methyl-D-Aspartate (NMDA) glutamate receptor and protein kinase Cγ (*PKC*γ) on alcohol drinking in wild-type mice. In addition, we investigated *in vivo* cAMP response element binding (CREB) activity using CRE-lacZ mice in an *ENT1*^{-/-} background.

Results—We identified that NMDA glutamate receptor-mediated down-regulation of intracellular *PKC*γ-neurogranin (Ng)-Ca²⁺-calmodulin dependent protein kinase type II (CaMKII) signaling is correlated with reduced CREB activity in *ENT1*^{-/-} mice. Inhibition of *PKC*γ promotes ethanol drinking in wild-type mice to levels similar to those of *ENT1*^{-/-} mice. In contrast, an NMDA glutamate receptor antagonist reduces ethanol drinking of *ENT1*^{-/-} mice.

© 2011 Society of Biological Psychiatry. Published by Elsevier Inc. All rights reserved.

Correspondence should be addressed to Dr. Doo-Sup Choi, Department of Molecular Pharmacology and Experimental Therapeutics, Mayo Clinic College of Medicine, 200 First Street SW, Rochester, Minnesota 55905, USA Phone: (507) 284-5602 Fax: (507) 266-0824 choids@mayo.edu.

⁵Present Address: Harvard Medical School, Boston, Massachusetts 02114

Publisher's Disclaimer: This is a PDF file of an unedited manuscript that has been accepted for publication. As a service to our customers we are providing this early version of the manuscript. The manuscript will undergo copyediting, typesetting, and review of the resulting proof before it is published in its final citable form. Please note that during the production process errors may be discovered which could affect the content, and all legal disclaimers that apply to the journal pertain.

Financial Disclosures

The authors reported no biomedical financial interests or potential conflicts of interest.

Conclusion—These findings demonstrate that the genetic deletion or pharmacological inhibition of ENT1 regulates NMDA glutamate receptor-mediated signaling in the NAc which provides a molecular basis that underlies the ethanol-preferring behavior of ENT1^{-/-} mice.

Keywords

Alcoholism; nucleus accumbens; ENT1; NMDA glutamate receptor; CGP37849; CREB

Introduction

Alcohol use disorders impose major public health and social problems with substantial worldwide economic loss (1) and cause approximately 85,000 deaths in the United States every year (2). Adenosine signaling has been implicated in the pathophysiology of several neuropsychiatric disorders including alcoholism (3–6). Initially, acute ethanol treatment increases extracellular adenosine in cultured cells by selectively inhibiting type 1 equilibrative nucleoside transporter (ENT1), while chronic ethanol exposure no longer increases extracellular adenosine levels owing to the downregulation of ENT1 gene expression (7). Consequently, reduced adenosine signaling has been implicated in decreased sensitivity (ataxia/hypnosis) to the intoxicating effect of ethanol as well as increased ethanol drinking mice (8). Mice lacking ENT1 (ENT1^{-/-}) display similar behaviors as chronic ethanol-treated or alcohol-preferring mice (9), as ENT1^{-/-} mice consume more alcohol and exhibit reduced sensitivity (ataxia/hypnosis) to acute ethanol exposure (10, 11). In contrast, mice over-expressing human ENT1 are more sensitive to the acute intoxicating effects of ethanol (12). Additionally, several recent animal studies further illustrate that ENT1 gene expression is inversely correlated with ethanol drinking (13–15). Furthermore, recent human genetic association studies demonstrated that variants of ENT1 are associated with an alcohol abuse phenotype in women (16), alcoholics with a history of withdrawal seizures (17) and heroin addiction (18). Therefore, the mechanistic understanding of how ENT1 contributes to alcoholism is important for the development of novel therapeutics.

One of the neural mechanisms underlying increased alcohol preference of ENT1^{-/-} mice involves increased glutamate neurotransmission in the nucleus accumbens (NAc) (10, 11). Inhibition of adenosine A1 receptors increases glutamate-evoked postsynaptic activity in the NAc (19) while activation of adenosine A₁ receptor reduces ethanol consumption in ENT1^{-/-} mice (10), suggesting that increased glutamate levels and ethanol consumption might be related to diminished adenosine A₁ receptor activity in ENT1^{-/-} mice. In addition, our recent study suggests that decreased synaptic glutamate uptake, owing to the reduction of ENT1-dependent excitatory amino acid transporter type 2 (EAAT2) expression or function in astrocytes (20), might contribute to increased glutamate levels in the NAc. Moreover, using *in vivo* magnetic resonance spectroscopy (MRS), we found that total glutamate levels are increased in the NAc of ENT1^{-/-} mice (21). Thus, it appears that the deficiency of ENT1 gene expression increases accumbal glutamate levels. However, the consequences of constitutively increased glutamate levels on postsynaptic signaling molecules in the NAc of ENT1^{-/-} mice remain unknown.

Here we show that accumbal *N*-methyl-D-aspartate (NMDA) glutamate receptor (NMDAR)-mediated cAMP response element binding (CREB) activity *via* protein kinase Cγ (PKCγ) regulates ethanol drinking behaviors of ENT1^{-/-} mice. Our findings provide a novel signaling pathway, which might link increased glutamate signaling and decreased CREB activity with excessive ethanol drinking in mice.

Materials and Methods

See Supplement 1 for detailed methods

Animal

ENT1^{-/-} mice were generated as described (10). We used F2 generation hybrid mice with a C57BL/6J × 129X1/SvJ genetic background. We crossed CRE-lacZ mice in a C57BL/6J background with ENT1^{-/-} mice in a C57BL/6J background, then crossed the CRE-lacZ/ENT1^{+/-} with ENT1^{+/-} mice in a 129X1/SvJ background to generate CRE-lacZ/ENT1^{+/+} or CRE-lacZ/ENT1^{-/-} mice. We used 8–16 week old male littermates for all experiments.

Microdialysis

Animals were anesthetized with ketamine/xylazine (100 and 15 mg/kg, *i.p.*; Sigma, MO) and placed in a digital stereotaxic alignment system (Model 1900, David Kopf Instruments, CA). Guide cannulae were implanted into the NAc (AP: 1.3 mm; ML: 0.5 mm; DV: -3.5 mm; Figure S1A in Supplement 1 for the location of microdialysis probes) as described (11). To confirm the extracellular glutamate concentration in the NAc, we employed a no-net flux microdialysis experiment. Vehicle (Ringer's) solution, 0.5, 1.0, and 5.0 μM glutamate solutions were circulated in the microprobe and equilibrated with extracellular glutamate. Glutamate concentrations were quantified using HPLC-ECD (HTEC-500, Eicom, Kyoto, Japan). After the microdialysis experiment, we confirmed the location of microdialysis probes histologically (Figure S1 in Supplement 1).

NAc Protein Profiling Using Proteomics

We pooled the same amount of NAc proteins from 5 mice per genotype (10 mice/iTRAQ experiment). We performed three independent iTRAQ experiments with different sets of mice and duplicated each sample for LC/MS/MS analysis. For iTRAQ labeling, trypsin-digested peptides were purified and desalted using an Oasis HLB extraction kit (22, 23). Concentrated peptides were reconstituted in iTRAQ reagents for 2-plex reactions (114 = ENT1^{+/+} mice; 116 = ENT1^{-/-} mice). The peptides were then analyzed by nanoLC-LTQ Orbitrap mass spectrometry (Thermo Fisher Scientific, Waltham, MA) (Figure S2A in Supplement 1). We validated the iTRAQ results using 3 different methods. 1) To verify the technical and experimental variation of iTRAQ reactions, we used an internal standard (ISTD) peptide as a reaction control. 2) We normalized the bias of each iTRAQ reaction using two house-keeping genes, GAPDH and beta-tubulin. 3) In addition, we verified the biological variation of each sample by examining peptide levels (peptidomics) using an iTRAQ method (Figure S2B in Supplement 1).

Protein Phosphatase Activity Assay

Cytoplasmic protein (2 μg) from the NAc was used for phosphatase assay (Enzo Life Sciences Inc., PA). Released phosphates were reacted with BIOMOL GREEN™ reagent (Enzo Life Sciences Inc., PA) and detected in OD 620 nm using a microplate reader (Thermo Fisher Scientific Inc., Waltham, MA).

Western Blot Analysis

Brains were quickly removed and dissected to isolate the NAc. Briefly, tissues were homogenized in a solution containing 50 mM Tris buffer (pH 7.4), 2 mM EDTA, 5 mM EGTA, 0.1% SDS, protease inhibitor cocktail (Roche), and phosphatase inhibitor cocktail type I and II (Sigma). Homogenates were centrifuged at 500 g at 4°C for 15 min and supernatants were collected. Proteins were separated by 4–12% NuPAGE™ Bis Tris gels at 130 V for 2 h, transferred onto PVDF membranes at 30 V for 1 h (Invitrogen), and incubated

with antibodies listed in the Supplement 1. Protein levels were normalized by GAPDH and quantified compared to the control group.

X-gal Staining for Measurement of CREB Activity

CRE-lacZ mice were rapidly dissected into cold fixative solution (2% paraformaldehyde, 0.2% glutaraldehyde in PBS) and fixed overnight at 4°C. Coronal cryostat sections (40 μm) were cut and washed for 5 min, three times, with PBS and then incubated overnight at 37°C in the reaction solution (1 mg/ml X-gal, 5 mM potassium ferricyanide, 5 mM potassium ferrocyanide, 2 mM MgCl₂ in PBS) in a dark tray. The number of X-gal positive cells was counted in the regions of interest (0.15 mm²) using a Leica DM4000B microscope.

Effect of PKC Inhibitor Microinjection or CGP37849 Administration on Ethanol Drinking

Oral alcohol self-administration was examined using a two-bottle choice experiment (10, 24). Male mice were trained to self-administer 10% ethanol (w/v) orally. To examine the effect of PKC inhibition on ethanol drinking, 1.0, 10 or 20 μM of PKC inhibitor 19–31 (Calbiochem, CA) was bilaterally microinjected into the NAc (AP: 1.3 mm; ML: ± 1.5 mm; DV: –3.5 mm; Figure S1B in Supplement 1 for the location of microinjection cannulae) for 4 d during the 10% ethanol drinking session. To examine the effect of CGP37849 (NMDA glutamate receptor-specific antagonist, TOCRIS, Ellisville, MO) on ethanol drinking, a new group of mice was given saline, 1.0, 5.0 and 10 mg/kg CGP37849 (*i.p.*) for 4 d during the 10% ethanol drinking session.

Statistical Analysis

Data are presented as mean ± SEM (standard error of the mean). Statistical analyses were performed using unpaired two-tailed *t*-test (Prism v 4, GraphPad Software, La Jolla, CA), one-way, or two-way repeated measures ANOVA (SigmaStat v 3.1, Systat Software, Point Richmond, CA). Results were considered significantly different when *p* < 0.05.

Results

Increased Glutamate Levels in the NAc of ENT1^{-/-} Mice

We used microdialysis to investigate the effect of ENT1 deletion on extracellular adenosine and glutamate levels in the NAc. In dialysates, adenosine levels were significantly decreased in the NAc of ENT1^{-/-} mice compared to ENT1^{+/+} mice (Figure 1A). Since adenosine receptor signaling has an effect on presynaptic glutamate release (10), we investigated extracellular glutamate concentrations using microdialysis. The NAc of ENT1^{-/-} mice showed increased basal glutamate levels compared to ENT1^{+/+} mice (Figure 1B). Since the recovery rate of the microdialysis probe is around 10–15% and the dialysis efficiency depends on changes in analytes, extracellular glutamate levels in NAc were confirmed using a no-net flux microdialysis method (25). We determined that extracellular glutamate concentrations were significantly increased by about 2.6-fold in ENT1^{-/-} mice (Figure 1C), which is consistent with our previous electrophysiology study (10).

Since EAAT1 and EAAT2 are mainly responsible for the uptake of extracellular glutamate in the striatum (26, 27), we examined both EAAT1 and EAAT2 expression in the NAc of ENT1^{-/-} mice. EAAT2 levels were decreased in ENT1^{-/-} mice compared to ENT1^{+/+} mice (Figure 1D) while EAAT1 levels were similar between genotypes (Figure 1E) by Western blot analysis. Consistently, our recent study demonstrated that inhibition of ENT1 expression or function led to decreased EAAT2 expression or activity in glutamate uptake in astrocytes (20).

Proteomics Revealed Altered NMDA Glutamate Receptor Signaling Proteins in the NAc of ENT1^{-/-} Mice

Since numerous signaling pathways are involved in glutamate-mediated signaling (28), we employed a proteomic technique, iTRAQ (29, 30), to elucidate proteome changes in the NAc of ENT1^{-/-} mice. We identified 533 accumbal proteins, both digested peptides and endogenous accumbal peptides, and quantified the iTRAQ reporter ions (Figure S2B,C in Supplement 1). Three independent experiments revealed that 5 signaling proteins were significantly changed in the NAc of ENT1^{-/-} mice compared to ENT1^{+/+} mice (Table 1) while other signaling proteins were unaltered (Table S1 in Supplement 1). Particularly, we found that neurogranin (Ng) and calmodulin (CaM), which are essential components of NMDAR-mediated signaling (31), were significantly increased in the NAc of ENT1^{-/-} mice. We also observed decreased EAAT2 expression, but not EAAT1, in the NAc of ENT1^{-/-} mice (Table S1 in Supplement 1).

Altered NMDAR Signaling in the NAc of ENT1^{-/-} Mice

Our proteomic approach led us to examine the expression of NMDAR subunits and their phosphorylated forms using Western blot analysis because we observed that several NMDAR-dependent signaling molecules were significantly altered in the NAc of ENT1^{-/-} mice. Interestingly, we found that phospho-NR1 (Ser890), which is preferentially phosphorylated by PKC γ (32), is decreased in the NAc of ENT1^{-/-} mice (Figure S3A in Supplement 1). Other NMDAR subunits and α -amino-3-hydroxy-5-methyl-4-isoxazolepropionic acid receptor (AMPA) subunits (Figure S3A,B in Supplement 1) were not changed between genotypes. These results indicate that constitutively increased glutamate levels in the NAc could alter NMDA-dependent glutamate signaling in postsynaptic neurons of ENT1^{-/-} mice.

We confirmed that Ng protein levels were increased in the NAc of ENT1^{-/-} mice compared to ENT1^{+/+} mice (Figure 2A). Since phosphorylation on the IQ motif (26–47) of Ng *via* PKC γ is known to regulate Ca²⁺-CaM dependent protein kinase (CaMK) activity (33–35), we examined pNg (Ser36) levels, an active form of Ng, in the NAc. Surprisingly, pNg (Ser36) levels were significantly decreased in ENT1^{-/-} mice compared to ENT1^{+/+} mice (Figure 2A and Figure S4A in Supplement 1). Since PKC γ phosphorylates both Ng (Ser36) and NR1 (Ser890), we examined pPKC γ (Thr514), an active form of PKC γ . Consistently, pPKC γ (Thr514) levels were significantly reduced in ENT1^{-/-} mice compared to ENT1^{+/+} mice, while total PKC γ levels were similar between genotypes (Figure 2A and Figure S4A in Supplement 1).

Increased pNg (Ser36) levels are known to promote dissociation of Ng from CaM and increases Ca²⁺-CaM formation (35–38). Thus, decreased pNg (Ser36) and pPKC γ (Thr514) or increased Ng might decrease Ca²⁺-CaM formation due to increased CaM-Ng binding. This could decrease CaMK activity including that of CaMK type II (CaMKII), which is highly expressed in dendritic spines (39). As expected, we found that levels of pCaMKII (Thr286), an active form of CaMKII, were significantly reduced while no changes in total CaMKII expression levels were observed between genotypes. We also found that CaM levels in the NAc were not altered in ENT1^{-/-} mice (Figure 2A).

Increased PP1/PP2A Activity in the NAc of ENT1^{-/-} Mice

Next, we investigated phosphatase activity since phosphorylation of key signaling proteins involved in NMDAR-mediated signaling were decreased in the NAc. Because PP1/PP2A is known to dephosphorylate pPKC γ (Thr514), while PP2B (calcineurin) dephosphorylates pNg (Ser36) (40), we examined the activity of these phosphatases. We found that PP1/PP2A activity was significantly increased while there were no differences in PP2B (calcineurin)

activity in the NAc of $ENT1^{-/-}$ mice (Figure 2B), suggesting that increased PP1/PP2A activity is related to decreased pPKC γ (Thr514) levels, which could thereby result in reduced pNg (Ser36) in the NAc.

Reduced CREB Activity in $ENT1^{-/-}$ Mice

Since reduced pCaMKII (Thr286) levels or CaMK activity could alter gene expression *via* CREB activity (41), we examined the levels of CREB and pCREB (Ser133), an active form of CREB, in the NAc. Interestingly, pCREB (Ser133) levels were decreased while CREB levels were not changed (Figure 3A,B and Figure S4A in Supplement 1). Next, to further investigate whether *in vivo* CREB activity is altered in $ENT1^{-/-}$ mice, we generated mice expressing β -galactosidase (lacZ) under the control of seven-repeated CRE sites in an $ENT1^{+/+}$ or $ENT1^{-/-}$ background (CRE-lacZ/ $ENT1^{+/+}$ or CRE-lacZ/ $ENT1^{-/-}$). Consistent with Western blot analysis, we found that the lacZ expression in the NAc core region was significantly decreased in CRE-lacZ/ $ENT1^{-/-}$ compared to CRE-lacZ/ $ENT1^{+/+}$ mice (Figure 3C), while no significant difference in the NAc shell region was observed between genotypes (Figure S5 in Supplement 1).

ENT1 Inhibition Decreases CREB Activity in the NAc

Next, we examined whether microinjection of ENT1-specific inhibitor NBTI (nitrobenzylthioinosine) into the NAc reduces CREB activity in $ENT1^{+/+}$ mice. Because CREB activity is altered 2–3 h after an ethanol injection in the NAc (Figure S6 in Supplement 1), we examined CREB activity 2 h after the NBTI microinjection (50 μ M). As shown in Figure 3D, we observed reduced CREB activity in the NAc core of CRE-lacZ/ $ENT1^{+/+}$ mice by NBTI microinjection, while no significant changes in CRE-lacZ/ $ENT1^{-/-}$ mice were observed (Figure 3E). Together with the data from $ENT1^{-/-}$ mice (Figure 3A–C), these results indicate that deficiency of ENT1 expression or function decreases CREB activity in the NAc core in mice.

Inhibition of PKC γ -Driven CaMKII and CREB Activity Increases Ethanol Consumption in $ENT1^{+/+}$ Mice, but not in $ENT1^{-/-}$ Mice

In addition, we examined the effect of PKC γ inhibition on CaMKII and CREB activities as well as ethanol drinking behavior. We microinjected a peptide inhibitor, which is known to inhibit PKC γ activity in the NAc (42). Our results showed that microinjection of 10 μ M of the peptide inhibitor in the NAc of $ENT1^{+/+}$ mice decreased pCaMKII (Figure 4A), suggesting that PKC γ activity regulates pCaMKII in the NAc. The same treatment also decreased CREB activity in the NAc core compared to its saline-treated group of CRE-lacZ/ $ENT1^{+/+}$ mice (Figure 4B). Furthermore, the bilateral microinjection with 10 μ M or 20 μ M of PKC inhibitor peptide for 4 d increased ethanol consumption (Figure 4C) and preference (Figure 4D) of $ENT1^{+/+}$ mice compared to saline-treated control mice. Interestingly, PKC inhibition in the NAc had no effect on ethanol consumption or preference of $ENT1^{-/-}$ mice. During saline treatment, $ENT1^{-/-}$ mice displayed increased ethanol consumption and preference compared to $ENT1^{+/+}$ mice (Figure 4C,D) as we have observed previously (10). One-way ANOVA analysis of ethanol consumption indicated that PKC inhibitor treatment displayed a dose effect [$F(3,29) = 3.3, p = 0.035$] in $ENT1^{+/+}$ mice, while no significant changes were observed in $ENT1^{-/-}$ mice [$F(3,25) = 0.4, p = 0.73$]. Similarly, for ethanol preference, one-way ANOVA showed a significant dose effect in $ENT1^{+/+}$ mice [$F(3,30) = 3.3, p = 0.03$], while no significant changes were observed in $ENT1^{-/-}$ mice [$F(3,26) = 0.2, p = 0.89$]. Water consumption was similar between genotypes during PKC inhibitor treatment (Figure S7A in Supplement 1). Taken together, these results suggest that decreased PKC γ activity may regulate excessive ethanol drinking in $ENT1^{-/-}$ mice.

NMDAR Antagonist CGP37849 Normalized the Decreased pPKC γ , pNg and pCaMKII levels in the NAc of ENT1^{-/-} Mice

Next, we investigated whether blocking the NMDAR could normalize the phosphorylation of signaling molecules in ENT1^{-/-} mice. We used a specific NMDAR antagonist CGP37849, which is known to reduce ethanol consumption (43). As shown in Figure 5A, systemic treatment of CGP37849 (10 mg/kg, *i.p.*) for 2 h normalized pPKC γ , pCaMKII, and pCREB levels in the NAc of ENT1^{-/-} mice to a level similar to that of ENT1^{+/+} mice (Figure S4B in Supplement 1). Their non-phosphorylated forms remained unchanged (data not shown). Interestingly, this CGP37849 treatment even reversed (up-regulated) pNg levels in ENT1^{-/-} mice compared to ENT1^{+/+} mice, suggesting that constitutively increased glutamate levels account for altered phosphorylation of these four key signaling molecules in ENT1^{-/-} mice. Our findings suggest that increased extracellular glutamate levels might decrease CREB activity through inhibiting PKC γ -driven pNg and pCaMKII levels in the NAc. In addition, increased PP1/PP2A activity in ENT1^{-/-} mice was normalized by CGP37849 (Figure 5B). Thus, glutamate signaling *via* NMDAR may be essential in PKC γ -driven pNg and pCaMKII regulation in ENT1^{-/-} mice.

CaMKII Inhibition Blocks the Normalization Effect on CREB Activity by CGP37849

Although CGP37849 normalized several signaling molecules in ENT1^{-/-} mice, the link between glutamate signaling and CaMKII-mediated signaling remained unclear. To investigate whether glutamate signaling *via* CaMKII regulates CREB activity, we examined the effect of CGP37849 treatment in conjunction with a CaMK-specific inhibitor, KN93, which is known to inhibit CaMKII by systemic injection (44). Mice were treated with 15 mg/kg KN93 (*i.p.*) 30 min before 10 mg/kg CGP37849 injection. While the levels of pNg, pPKC γ , and pCaMKII of ENT1^{-/-} mice were restored to those of ENT1^{+/+} mice 2 h following CGP37849 treatment, CREB activity remained significantly reduced in ENT1^{-/-} mice when KN93 was injected prior to CGP37849 (Figure S8 in Supplement 1). These results indicate that CaMKII signaling regulates CREB activity in the NAc of ENT1^{-/-} mice.

CGP37849 Treatment Reduces Ethanol Self-Administration

Finally, we examined whether NMDAR antagonist CGP37849 treatment reduces ethanol consumption or preference using a two-bottle choice drinking experiment when mice were consistently drinking 10% ethanol. Before CGP37849 treatment, ENT1^{-/-} mice showed increased basal ethanol consumption and preference compared to ENT1^{+/+} mice as we reported previously (10). During the CGP37849 injection session, both ENT1^{+/+} and ENT1^{-/-} mice showed significantly decreased ethanol consumption and preference compared to their respective saline-injection session (Figure 5C,D). For ethanol consumption, two-way repeated measures ANOVA indicated a significant effect of genotype [$F(1,119) = 15.3, p < 0.001$] and CGP37849 doses [$F(4,119) = 8.4, p < 0.001$] on ethanol consumption. For ethanol preference, two-way repeated measures ANOVA showed significant effects of genotype [$F(1,118) = 4.5, p = 0.046$] and CGP37849 doses [$F(4,119) = 6.6, p < 0.001$] on preference. Water consumption was similar between genotypes during CGP37849 treatment (Figure S7B in Supplement 1). These results are consistent with previous findings that the inhibition of NMDAR reduces ethanol preference (45).

Discussion

We identified that deletion of ENT1 induces a decrease of extracellular adenosine levels and an increase of extracellular glutamate levels in the NAc by microdialysis. Our proteomic study has revealed an essential signaling pathway elucidating adenosine-regulated glutamate signaling in ENT1^{-/-} mice, which appears to alter CREB activity and ethanol drinking, as

summarized in Figure S9 (Supplement 1). It is noteworthy that excitatory amino acid transporter 2 (EAAT2), neurogranin (Ng), and calmodulin (CaM), which regulate glutamate levels or NMDAR signaling (31), showed changes in expression in the NAc.

Our functional studies suggest that decreased PKC γ -dependent pNg (Ser36) and Ca²⁺-CaM dependent kinase II (CaMKII) activity regulate CREB activity in the NAc of ENT1^{-/-} mice. Since PKC γ ^{-/-} mice show reduced acute intoxicating effects of ethanol (46, 47), similar to ENT1^{-/-} mice (10), reduced PKC γ activity might be correlated with increased glutamate signaling in ENT1^{-/-} mice. Although further experiments are required to reveal how increased NMDAR signaling is causally related to decreased pPKC γ , our study suggested that increased PP1/PP2A activity could decrease pPKC γ levels (40) in the NAc. As a CaM binding protein, Ng is essential for Ca²⁺ release from the Ca²⁺-CaM complex in the postsynaptic neurons. Especially, Ng regulates the availability of CaM through PKC γ -dependent phosphorylation of serine 36 within the IQ motif of Ng (33, 34, 48). While non-phosphorylated Ng strongly binds to CaM, pNg (Ser36) blocks the formation of Ng-CaM complex (49). It remains unclear why total Ng levels were increased in ENT1^{-/-} mice, however, it might be owing to a compensatory response to normalize altered NMDAR signaling. Nevertheless, consistent with our finding, a recent study revealed that pNg is inversely correlated with Ng levels (50). Interestingly, chronic ethanol administration is known to increase Ng levels in the brain, particularly in the hippocampus (51, 52). Moreover, two other studies showed that Ng negatively modulates CaM and inhibits Ca²⁺-CaM signaling (52, 53), indicating that reduced pNg or increased Ng levels are essential in the reduction of Ca²⁺-CaM signaling in ENT1^{-/-} mice. CaMKII modulates the interaction between glutamate and dopamine signaling in the NAc, which controls the behavioral sensitivity to cocaine and induces the cocaine-seeking behavior in rats (54, 55). Consistently, CaMKII levels were decreased in alcohol-preferring rats (56), but up-regulated in the NAc of alcohol non-preferring rats (57), suggesting that decreased CaMK-dependent signaling is correlated with increased alcohol drinking.

It seemed paradoxical that both a hyper-glutamatergic state (58) and hypo-CREB activity (59) are known to be associated with alcohol use disorders, as increased glutamate receptor signaling is likely to increase CREB activity *via* several signaling mechanisms (28). Interestingly, CREB heterozygous mice (CREB^{+/-}) express reduced CREB and pCREB (Ser133) in the brain and prefer more alcohol in a two-bottle choice experiment (59). In this study, we found that CREB expression levels are not changed while pCREB (Ser133) levels are decreased in the NAc of ENT1^{-/-} mice. Because of lower baseline pCREB levels in ENT1^{-/-} mice, our previous slope comparison between CREB and pCREB along with increased protein amounts in Western blot, were interpreted as an increased pCREB/CREB ratio in ENT1^{-/-} mice (10). However, we validated CREB activity using CRE-lacZ/ ENT1^{-/-} mice, which revealed that *in vivo* CREB activity is reduced in the NAc core region, but not in the NAc shell region.

Pharmacological inhibition of accumbal ENT1 by microinjection of an ENT1-specific inhibitor also reduced CREB activity, suggesting that CREB activity is dependent upon ENT1 function. Several key molecular changes contributing to reduced CREB activity in ENT1^{-/-} mice were reversed by an NMDAR-specific antagonist, CGP37849. Interestingly, inhibition of CaMKII activity by KN93 (44) blocked the effect of CGP37849 treatment on CREB activity. Furthermore, daily treatment of CGP37849 for four days reduced ethanol consumption and preference in ENT1^{-/-} and ENT1^{+/+} mice, suggesting that increased NMDAR signaling *via* decreased activity of CaMKII and CREB are involved in increased ethanol consumption in ENT1^{-/-} mice. Consistent with our finding, CGP37849 (2–8 mg/kg, *i.p.*) administration reduces alcohol intake after alcohol deprivation in mice (43). Although there were no differences in water consumption between genotypes or between CGP37849

treatments (Figure S7B in Supplement 1), the 7–9% lower body weight of ENT1^{-/-} mice compared to ENT1^{+/+} mice (10) may have contributed to the difference between ethanol consumption and preference when comparing genotypes.

The NAc core region primarily regulates the motivational effects of conditioned stimuli (60), suggesting that reduced CREB activity in the NAc core of ENT1^{-/-} mice might account for increased ethanol drinking (10, 11). Since the shell region of the NAc appears to regulate reward response to addictive substances including alcohol (60), similar CREB activity in the shell region might be a reason contributing to the lack of a difference in ethanol-induced conditioned place preference between ENT1^{-/-} and ENT1^{+/+} mice (11).

In summary, the molecular characterization of the NAc using microdialysis and proteomics provides a possible signaling pathway that demonstrates how the deletion of ENT1, resulting in increased extracellular glutamate, alters NMDAR signaling and decreases CREB activity *via* a reduction of pPKC γ . Together, our study offers a novel role of adenosine-regulated glutamate signaling on CREB activity, which controls ethanol-drinking behaviors in mice.

Supplementary Material

Refer to Web version on PubMed Central for supplementary material.

Acknowledgments

This work was supported by the Samuel Johnson Foundation for Genomics of Addiction Program at Mayo Clinic and by grants from the National Institutes of Health (NIH) to D.-S. C. (R01 AA015164 and R01 AA018779). H.W.N. received postdoctoral fellowship (C00088) from Korea Research Foundation.

We thank D. Frederixson, D. Walker, and C. Ruby for their help in preparing the manuscript. We thank Dr. Eric Nestler (Mount Sinai School of Medicine) for providing CRE-lacZ mice and helpful comments on the manuscript. The CRE-lacZ mice were made in Dr. Jerry Chi-Ping Yin's Laboratory.

References

1. Harwood HJ, Fountain D, Livermore G. Economic costs of alcohol abuse and alcoholism. *Recent Dev Alcohol*. 1998; 14:307–330. [PubMed: 9751951]
2. Mokdad AH, Marks JS, Stroup DF, Gerberding JL. Actual causes of death in the United States, 2000. *JAMA*. 2004; 291:1238–1245. [PubMed: 15010446]
3. Asatryan L, Nam HW, Lee MR, Thakkar MM, Dar MS, Davies DL, et al. Implication of the Purinergic System in Alcohol Use Disorders. *Alcohol Clin Exp Res*. 2010 In Press.
4. Dunwiddie TV, Masino SA. The role and regulation of adenosine in the central nervous system. *Annu Rev Neurosci*. 2001; 24:31–55. [PubMed: 11283304]
5. Fredholm BB, Chen JF, Masino SA, Vaugeois JM. Actions of adenosine at its receptors in the CNS: insights from knockouts and drugs. *Annu Rev Pharmacol Toxicol*. 2005; 45:385–412.
6. Ferré S, Fredholm BB, Morelli M, Popoli P, Fuxe K. Adenosine-dopamine receptor-receptor interactions as an integrative mechanism in the basal ganglia. *Trends Neurosci*. 1997; 20:482–487. [PubMed: 9347617]
7. Nagy LE, Diamond I, Casso DJ, Franklin C, Gordon AS. Ethanol increases extracellular adenosine by inhibiting adenosine uptake via the nucleoside transporter. *J Biol Chem*. 1990; 265:1946–1951. [PubMed: 2298733]
8. Ruby CL, Adams C, Knight EJ, Nam HW, Choi DS. An Essential Role for Adenosine Signaling in Alcohol Abuse. *Curr Drug Abuse Rev*. 2010; 3:163–174. [PubMed: 21054262]
9. Melendez RI, Kalivas PW. Last call for adenosine transporters. *Nat Neurosci*. 2004; 7:795–796. [PubMed: 15280889]

10. Choi DS, Cascini MG, Mailliard W, Young H, Paredes P, McMahon T, et al. The type 1 equilibrative nucleoside transporter regulates ethanol intoxication and preference. *Nat Neurosci*. 2004; 7:855–861. [PubMed: 15258586]
11. Chen J, Nam HW, Lee MR, Hinton DJ, Choi S, Kim T, et al. Altered glutamatergic neurotransmission in the striatum regulates ethanol sensitivity and intake in mice lacking ENT1. *Behav Brain Res*. 2010; 208:636–642. [PubMed: 20085785]
12. Parkinson FE, Xiong W, Zamzow CR, Chestley T, Mizuno T, Duckworth ML. Transgenic expression of human equilibrative nucleoside transporter 1 in mouse neurons. *J Neurochem*. 2009; 109:562–572. [PubMed: 19222701]
13. Short JL, Drago J, Lawrence AJ. Comparison of ethanol preference and neurochemical measures of mesolimbic dopamine and adenosine systems across different strains of mice. *Alcohol Clin Exp Res*. 2006; 30:606–620. [PubMed: 16573578]
14. Bell RL, Kimpel MW, McClintick JN, Strother WN, Carr LG, Liang T, et al. Gene expression changes in the nucleus accumbens of alcohol-preferring rats following chronic ethanol consumption. *Pharmacol Biochem Behav*. 2009; 94:131–147. [PubMed: 19666046]
15. Sharma R, Engemann S, Sahota P, Thakkar MM. Role of adenosine and wake-promoting basal forebrain in insomnia and associated sleep disruptions caused by ethanol dependence. *J Neurochem*. 2010; 115:782–794. [PubMed: 20807311]
16. Gass N, Ollila HM, Utge S, Partonen T, Kronholm E, Pirkola S, et al. Contribution of adenosine related genes to the risk of depression with disturbed sleep. *J Affect Dis*. 2010; 126:134–139. [PubMed: 20392501]
17. Kim J-H, Karpayk VM, Biernacka JM, Nam HW, Lee MR, Preuss U, et al. Functional role of the polymorphic 647 T/C variant of ENT1 (SLC29A1) and its association with alcohol withdrawal seizure. *PLoS One*. 2010 In Press.
18. Levran O, Londono D, O'Hara K, Randesi M, Rotrosen J, Casadonte P, et al. Heroin addiction in African Americans: a hypothesis-driven association study. *Genes Brain Behav*. 2009; 8:531–540. [PubMed: 19500151]
19. Harvey J, Lacey MG. A postsynaptic interaction between dopamine D1 and NMDA receptors promotes presynaptic inhibition in the rat nucleus accumbens via adenosine release. *J Neurosci*. 1997; 17:5271–5280. [PubMed: 9204911]
20. Wu J, Lee MR, Choi S, Kim T, Choi DS. ENT1 regulates ethanol-sensitive EAAT2 expression and function in astrocytes. *Alcohol Clin Exp Res*. 2010; 34:1110–1117. [PubMed: 20374202]
21. Lee MR, Hinton DJ, Wu J, Mishra PK, Port JD, Macura SI, et al. Acamprosate reduces ethanol drinking behaviors and alters the metabolite profile in mice lacking ENT1. *Neurosci Lett*. 2010 In Press.
22. Hu J, Qian J, Borisov O, Pan S, Li Y, Liu T, et al. Optimized proteomic analysis of a mouse model of cerebellar dysfunction using amine-specific isobaric tags. *Proteomics*. 2006; 6:4321–4334. [PubMed: 16800037]
23. Liu T, D'Mello V, Deng L, Hu J, Ricardo M, Pan S, et al. A multiplexed proteomics approach to differentiate neurite outgrowth patterns. *J Neurosci Methods*. 2006; 158:22–29. [PubMed: 16797718]
24. Choi DS, Wang D, Dadgar J, Chang WS, Messing RO. Conditional rescue of protein kinase C epsilon regulates ethanol preference and hypnotic sensitivity in adult mice. *J Neurosci*. 2002; 22:9905–9911. [PubMed: 12427847]
25. Szumlinski KK, Lominac KD, Kleschen MJ, Oleson EB, Dehoff MH, Schwarz MK, et al. Behavioral and neurochemical phenotyping of Homer1 mutant mice: possible relevance to schizophrenia. *Genes Brain Behav*. 2005; 4:273–288. [PubMed: 16011574]
26. Amara SG, Fontana AC. Excitatory amino acid transporters: keeping up with glutamate. *Neurochem Int*. 2002; 41:313–318. [PubMed: 12176072]
27. Chaudhry FA, Lehre KP, van Lookeren Campagne M, Ottersen OP, Danbolt NC, Storm-Mathisen J. Glutamate transporters in glial plasma membranes: highly differentiated localizations revealed by quantitative ultrastructural immunocytochemistry. *Neuron*. 1995; 15:711–720. [PubMed: 7546749]

28. Lonze BE, Ginty DD. Function and regulation of CREB family transcription factors in the nervous system. *Neuron*. 2002; 35:605–623. [PubMed: 12194863]
29. Bantscheff M, Boesche M, Eberhard D, Matthieson T, Sweetman G, Kuster B. Robust and sensitive iTRAQ quantification on an LTQ Orbitrap mass spectrometer. *Mol Cell Proteomics*. 2008; 7:1702–1713. [PubMed: 18511480]
30. Han CL, Chien CW, Chen WC, Chen YR, Wu CP, Li H, et al. A multiplexed quantitative strategy for membrane proteomics: opportunities for mining therapeutic targets for autosomal dominant polycystic kidney disease. *Mol Cell Proteomics*. 2008; 7:1983–1997. [PubMed: 18490355]
31. Xia Z, Storm DR. The role of calmodulin as a signal integrator for synaptic plasticity. *Nat Rev Neurosci*. 2005; 6:267–276. [PubMed: 15803158]
32. Sanchez-Perez AM, Felipe V. Serines 890 and 896 of the NMDA receptor subunit NR1 are differentially phosphorylated by protein kinase C isoforms. *Neurochem Int*. 2005; 47:84–91. [PubMed: 15936117]
33. Mahoney CW, Seki K, Huang KP. Phosphorylation of MARCKS, neuromodulin, and neurogranin by protein kinase C exhibits differential responses to diacylglycerols. *Cell Signal*. 1995; 7:679–685. [PubMed: 8519597]
34. Gerendasy DD, Sutcliffe JG. RC3/neurogranin, a postsynaptic calpacitin for setting the response threshold to calcium influxes. *Mol Neurobiol*. 1997; 15:131–163. [PubMed: 9396008]
35. Wu J, Huang KP, Huang FL. Participation of NMDA-mediated phosphorylation and oxidation of neurogranin in the regulation of Ca²⁺- and Ca²⁺/calmodulin-dependent neuronal signaling in the hippocampus. *J Neurochem*. 2003; 86:1524–1533. [PubMed: 12950461]
36. Dominguez-Gonzalez I, Vazquez-Cuesta SN, Algaba A, Diez-Guerra FJ. Neurogranin binds to phosphatidic acid and associates to cellular membranes. *Biochem J*. 2007; 404:31–43. [PubMed: 17295609]
37. Huang KP, Huang FL, Jager T, Li J, Reymann KG, Balschun D. Neurogranin/RC3 enhances long-term potentiation and learning by promoting calcium-mediated signaling. *J Neurosci*. 2004; 24:10660–10669. [PubMed: 15564582]
38. Krucker T, Siggins GR, McNamara RK, Lindsley KA, Dao A, Allison DW, et al. Targeted disruption of RC3 reveals a calmodulin-based mechanism for regulating metaplasticity in the hippocampus. *J Neurosci*. 2002; 22:5525–5535. [PubMed: 12097504]
39. Kennedy MB. Signal transduction molecules at the glutamatergic postsynaptic membrane. *Brain Res Brain Res Rev*. 1998; 26:243–257. [PubMed: 9651538]
40. Seki K, Chen HC, Huang KP. Dephosphorylation of protein kinase C substrates, neurogranin, neuromodulin, and MARCKS, by calcineurin and protein phosphatases 1 and 2A. *Arch Biochem Biophys*. 1995; 316:673–679. [PubMed: 7864622]
41. Wu GY, Deisseroth K, Tsien RW. Activity-dependent CREB phosphorylation: convergence of a fast, sensitive calmodulin kinase pathway and a slow, less sensitive mitogen-activated protein kinase pathway. *Proc Natl Acad Sci U S A*. 2001; 98:2808–2813. [PubMed: 11226322]
42. Chen C, Kano M, Abeliovich A, Chen L, Bao S, Kim JJ, et al. Impaired motor coordination correlates with persistent multiple climbing fiber innervation in PKC γ mutant mice. *Cell*. 1995; 83:1233–1242. [PubMed: 8548809]
43. Vengeliene V, Bachteler D, Danysz W, Spanagel R. The role of the NMDA receptor in alcohol relapse: a pharmacological mapping study using the alcohol deprivation effect. *Neuropharmacology*. 2005; 48:822–829. [PubMed: 15829254]
44. Sato K, Suematsu A, Nakashima T, Takemoto-Kimura S, Aoki K, Morishita Y, et al. Regulation of osteoclast differentiation and function by the CaMK-CREB pathway. *Nat Med*. 2006; 12:1410–1416. [PubMed: 17128269]
45. Krystal JH, Petrakis IL, Mason G, Trevisan L, D'Souza DC. N-methyl-D-aspartate glutamate receptors and alcoholism: reward, dependence, treatment, and vulnerability. *Pharmacol Ther*. 2003; 99:79–94. [PubMed: 12804700]
46. Bowers BJ, Owen EH, Collins AC, Abeliovich A, Tonegawa S, Wehner JM. Decreased ethanol sensitivity and tolerance development in gamma-protein kinase C null mutant mice is dependent on genetic background. *Alcohol Clin Exp Res*. 1999; 23:387–397. [PubMed: 10195808]

47. Harris RA, McQuilkin SJ, Paylor R, Tonegawa S, Wehner JM. Mutant mice lacking the γ isoform of protein kinase C show decreased behavioral actions of ethanol and altered function of γ -aminobutyrate type A receptors. *Proc Natl Acad Sci U S A*. 1995; 92:3658–3662. [PubMed: 7731960]
48. Represa A, Deloulme JC, Sensenbrenner M, Ben-Ari Y, Baudier J. Neurogranin: immunocytochemical localization of a brain-specific protein kinase C substrate. *J Neurosci*. 1990; 10:3782–3792. [PubMed: 2269883]
49. Gerendasy DD, Herron SR, Jennings PA, Sutcliffe JG. Calmodulin stabilizes an amphiphilic alpha-helix within RC3/neurogranin and GAP-43/neuromodulin only when Ca²⁺ is absent. *J Biol Chem*. 1995; 270:6741–6750. [PubMed: 7896819]
50. Zhabotinsky AM, Camp RN, Epstein IR, Lisman JE. Role of the neurogranin concentrated in spines in the induction of long-term potentiation. *J Neurosci*. 2006; 26:7337–7347. [PubMed: 16837580]
51. Boucheron C, Alfos S, Enderlin V, Husson M, Pallet V, Jaffard R, et al. Age-related effects of ethanol consumption on triiodothyronine and retinoic acid nuclear receptors, neurogranin and neuromodulin expression levels in mouse brain. *Neurobiol Aging*. 2006; 27:1326–1334. [PubMed: 16115698]
52. Krazem A, Mons N, Higuieret P, Jaffard R. Chronic ethanol consumption restores the age-related decrease in neurogranin mRNA level in the hippocampus of mice. *Neurosci Lett*. 2003; 338:62–66. [PubMed: 12565141]
53. Martzen MR, Slemmon JR. The dendritic peptide neurogranin can regulate a calmodulin-dependent target. *J Neurochem*. 1995; 64:92–100. [PubMed: 7528268]
54. Anderson SM, Famous KR, Sadri-Vakili G, Kumaresan V, Schmidt HD, Bass CE, et al. CaMKII: a biochemical bridge linking accumbens dopamine and glutamate systems in cocaine seeking. *Nat Neurosci*. 2008; 11:344–353. [PubMed: 18278040]
55. Liu XY, Mao LM, Zhang GC, Papasian CJ, Fibuch EE, Lan HX, et al. Activity-dependent modulation of limbic dopamine D3 receptors by CaMKII. *Neuron*. 2009; 61:425–438. [PubMed: 19217379]
56. Witzmann FA, Li J, Strother WN, McBride WJ, Hunter L, Crabb DW, et al. Innate differences in protein expression in the nucleus accumbens and hippocampus of inbred alcohol-preferring and -nonpreferring rats. *Proteomics*. 2003; 3:1335–1344. [PubMed: 12872235]
57. McBride WJ, Schultz JA, Kimpel MW, McClintick JN, Wang M, You J, et al. Differential effects of ethanol in the nucleus accumbens shell of alcohol-preferring (P), alcohol-non-preferring (NP) and Wistar rats: a proteomics study. *Pharmacol Biochem Behav*. 2009; 92:304–313. [PubMed: 19166871]
58. Spanagel R, Kiefer F. Drugs for relapse prevention of alcoholism: ten years of progress. *Trends in pharmacological sciences*. 2008; 29:109–115. [PubMed: 18262663]
59. Pandey SC, Roy A, Zhang H, Xu T. Partial deletion of the cAMP response element-binding protein gene promotes alcohol-drinking behaviors. *J Neurosci*. 2004; 24:5022–5030. [PubMed: 15163695]
60. Everitt BJ, Robbins TW. Neural systems of reinforcement for drug addiction: from actions to habits to compulsion. *Nat Neurosci*. 2005; 8:1481–1489. [PubMed: 16251991]

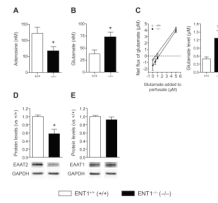


Figure 1.

Altered adenosine/glutamate levels in ENT1^{-/-} mice. **(A,B)** Measurement of adenosine and glutamate levels in the NAc. **(A)** ENT1^{-/-} mice showed decreased basal adenosine levels in accumbal dialysates [122.2 ± 18.5 nM in ENT1^{+/+} mice, 65.6 ± 14.8 nM in ENT1^{-/-} mice; $t(13) = 2.34$, $p = 0.03$]. $n = 7 \sim 8$ for each genotype. $*p < 0.05$ compared to ENT1^{+/+} mice by unpaired two-tailed t -test. **(B)** ENT1^{-/-} mice showed increased basal glutamate levels in accumbal dialysates [37.8 ± 8.3 nM in ENT1^{+/+} mice, 72.04 ± 11.0 nM in ENT1^{-/-} mice; $t(6) = 2.48$, $p = 0.04$]. $n = 4$ for each genotype. $*p < 0.05$ compared to ENT1^{+/+} mice by unpaired two-tailed t -test. $n = 4$ with duplicative analysis. **(C)** Measurement of extracellular glutamate concentration in the NAc using no-net flux microdialysis. ENT1^{-/-} mice showed a 2.6-fold increase in basal extracellular glutamate levels in the NAc [0.49 ± 0.08 nM in ENT1^{+/+} mice, 1.27 ± 0.29 nM in ENT1^{-/-} mice; $t(12) = 2.26$, $p = 0.04$]. $*p < 0.05$ compared to ENT1^{+/+} mice by unpaired two-tailed t -test. $n = 6 \sim 8$ for each genotype. **(D,E)** Expression of EAAT2 and EAAT1 in the NAc. **(D)** EAAT2 protein levels were significantly reduced in the NAc of ENT1^{-/-} mice compared to ENT1^{+/+} mice [$t(13) = 3.85$, $p = 0.002$], while **(E)** there was no difference in EAAT1 expression, $n = 7 \sim 8$, $*p < 0.05$ compared to ENT1^{+/+} mice after normalization by GAPDH (unpaired, two-tailed t -test). All data are presented as the mean ± SEM.

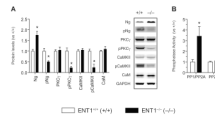


Figure 2.

Altered signaling molecules in the NAc of $ENT1^{-/-}$ mice. **(A)** Expression of signaling molecules in the NAc of $ENT1^{-/-}$ mice. Ng is increased [$t(14) = 3.95, p = 0.0015$] while pNg (Ser36) is reduced in $ENT1^{-/-}$ compared to $ENT1^{+/+}$ mice [$t(14) = 3.84, p = 0.002$]. PKC γ is not altered while pPKC γ (Thr514) is significantly reduced in $ENT1^{-/-}$ mice compared to $ENT1^{+/+}$ mice [$t(20) = 4.99, p < 0.001$]. CaMKII levels are similar while pCaMKII (Thr286) is significantly reduced in $ENT1^{-/-}$ mice compared to $ENT1^{+/+}$ mice [$t(14) = 2.51, p = 0.024$]. CaM levels are similar between genotypes. Representative blots and expression levels are expressed as fold change compared to $ENT1^{+/+}$ mice after normalization by GAPDH. $n = 8 \sim 11$ for each genotype; $*p < 0.05$ compared to $ENT1^{+/+}$ mice after normalization by GAPDH (unpaired, two-tailed t -test). **(B)** Altered protein phosphatase activity in the $ENT1^{-/-}$ mice. PP1/PP2A activity is increased in the NAc of $ENT1^{-/-}$ mice [$t(16) = 2.9, p = 0.02$], whereas PP2B (calcineurin) activity is not changed in the NAc. $n = 8 \sim 10$ for each genotype; $*p < 0.05$ compared to $ENT1^{+/+}$ mice by unpaired two-tailed t -test. All data are presented as mean \pm SEM.

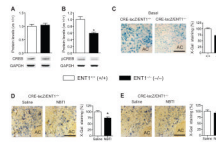


Figure 3.

In vivo CREB activity in ENT1^{-/-} mice. **(A)** No changes in CREB protein expression but **(B)** decreased phospho-CREB (Ser133) expression in ENT1^{-/-} mice by Western blot analysis [$t(14) = 4.8, p < 0.001$]. $n = 8$ for each genotype; $*p < 0.05$ compared to ENT1^{+/+} mice after normalization by GAPDH (unpaired, two-tailed t -test). **(C)** Representative NAc core coronal brain sections of β -galactosidase (lacZ) expression by X-Gal staining. Scale bar = 100 μ m. Decreased CRE-driven lacZ expression in the NAc core of CRE-lacZ/ENT1^{-/-} mice compared to CRE-lacZ/ENT1^{+/+} mice [$t(14) = 3.80, p = 0.002$]. $n = 8$ for each genotype; $*p < 0.05$ compared to CRE-lacZ/ENT1^{+/+} mice by unpaired two-tailed t -test. **(D, E)** Regulation of CREB activity by ENT1 inhibition. **(D)** CRE-lacZ/ENT1^{+/+} mice showed decreased CREB activity by ENT1 inhibition by 50 μ M NBTI microinjection to the NAc core [$t(18) = 3.7, p = 0.002$]. Representative NAc core coronal brain sections of lacZ expression after NBTI treatment by microinjection on CRE-lacZ/ENT1^{+/+} mice. Scale bar = 100 μ m. **(E)** CRE-lacZ/ENT1^{-/-} mice showed no further effects of ENT1 inhibition. Representative NAc core coronal brain sections of lacZ expression after NBTI treatment in CRE-lacZ/ENT1^{-/-} mice. Scale bar = 100 μ m. $n = 10$ for each genotype; $*p < 0.05$ compared to their saline-treated groups by unpaired two-tailed t -test. AC, anterior commissure. All data are presented as mean \pm SEM.

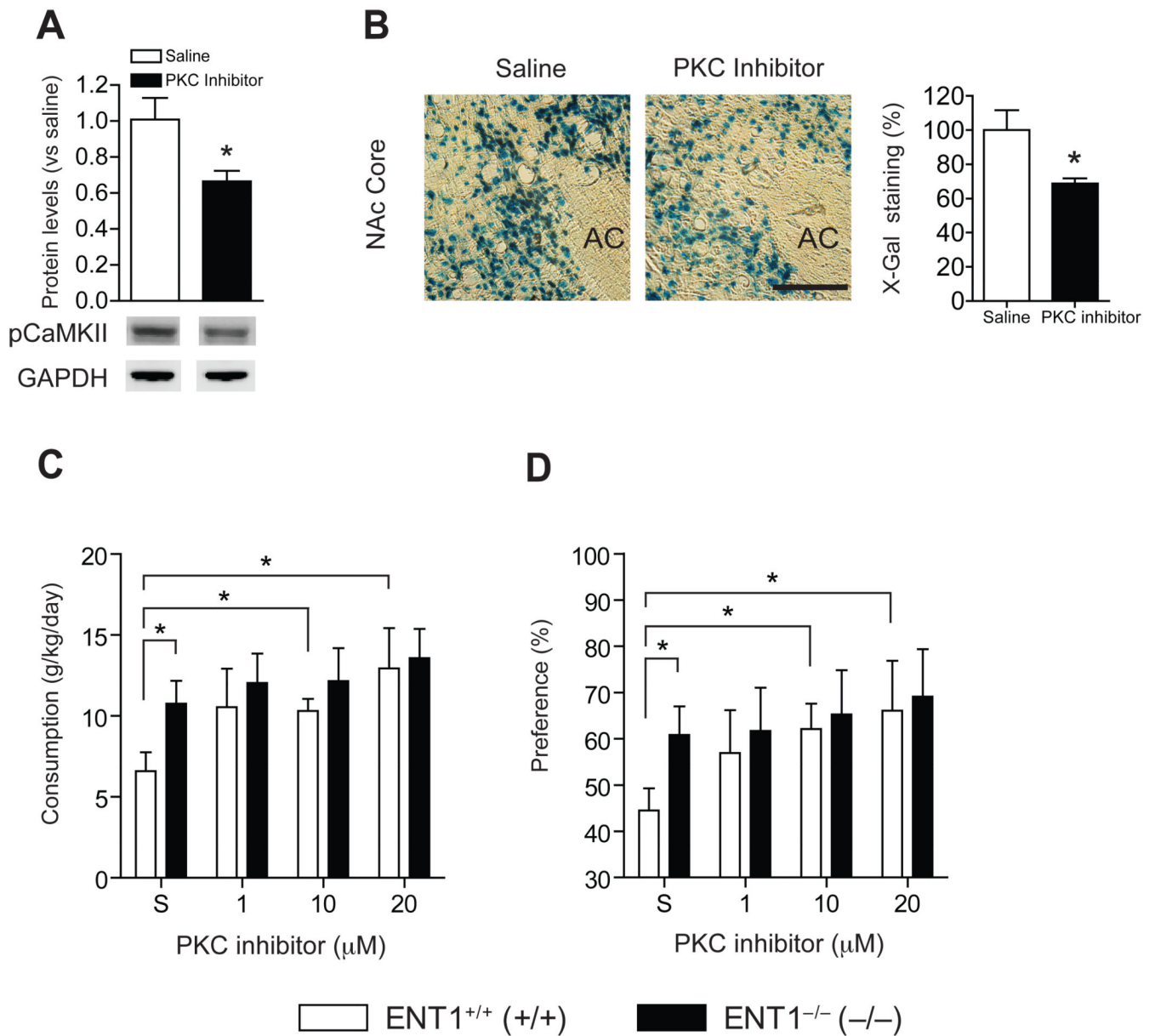


Figure 4. Effect of PKC γ inhibition on signaling and ethanol drinking behaviors in ENT1^{+/+} mice. **(A)** Microinjection of PKC inhibitor (10 μM) into the NAc reduced pCaMKII levels [$t(9) = 2.4$, $p = 0.04$] and **(B)** decreased lacZ expression in CRE-lacZ/ENT1^{+/+} mice [$t(10) = 2.6$, $p = 0.03$]. Representative coronal brain section of lacZ expression by X-gal staining. Scale bar = 100 μm . $n = 6$ for each genotype. Microinjection of PKC inhibitor (1.0, 10, and 20 μM) into the NAc elevated **(C)** ethanol consumption and **(D)** ethanol preference. ENT1^{+/+} mice showed increased ethanol drinking by PKC inhibition both in 10 μM [$t(16) = 2.2$, $p = 0.04$ for consumption, $t(17) = 2.1$, $p = 0.03$ for preference] and 20 μM [$t(16) = 2.7$, $p = 0.01$ for consumption, $t(16) = 2.13$, $p = 0.04$ for preference], but not in ENT1^{-/-} mice. $n = 8 \sim 9$ for each genotype. * $p < 0.05$ compared between treatment groups by unpaired two-tailed t -test. AC, anterior commissure. All data are presented as mean \pm SEM.

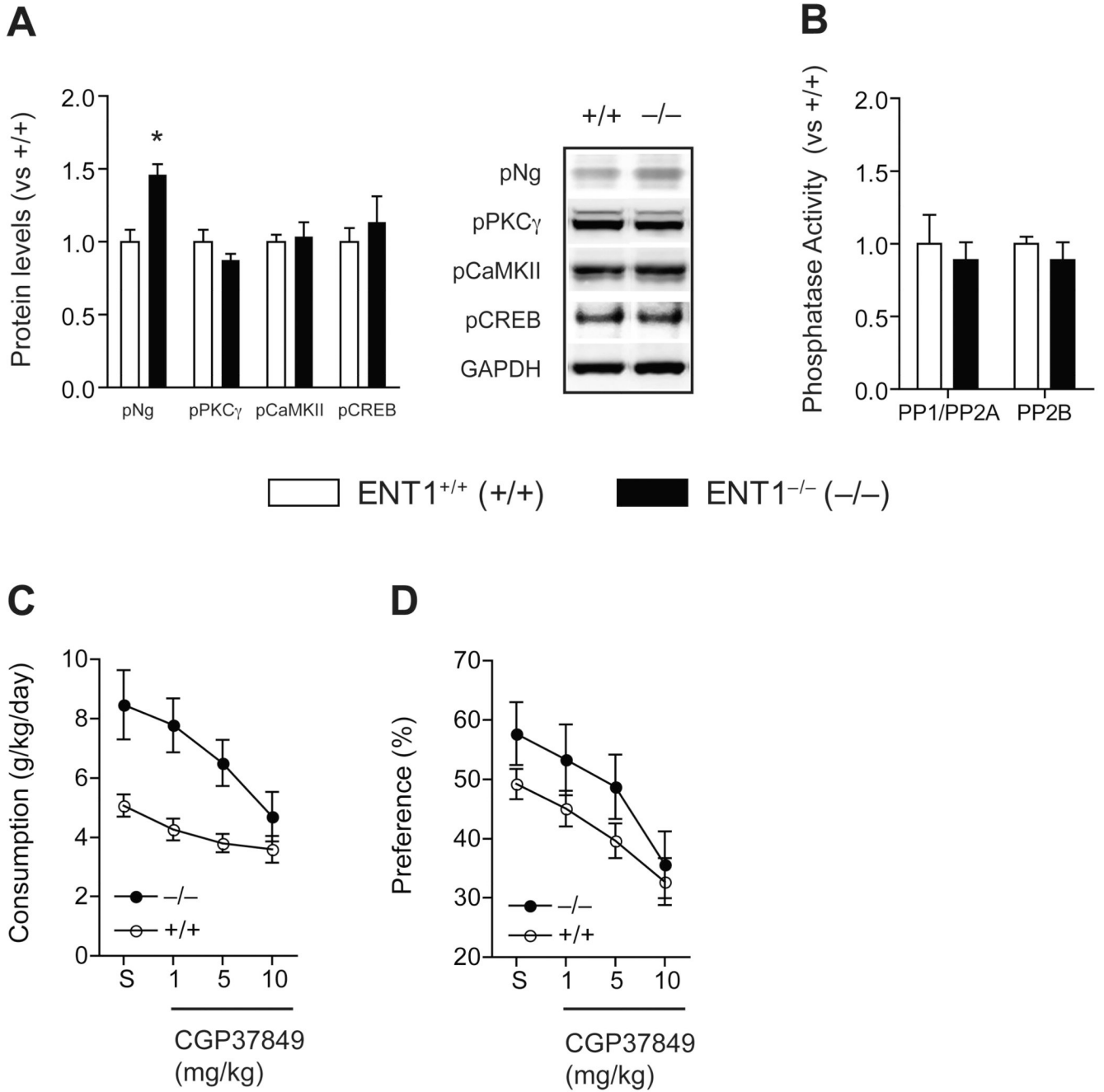


Figure 5. Effects of NMDAR antagonist CGP37849 in molecular signaling and ethanol drinking. **(A)** NMDA glutamate receptor antagonist CGP37849 (10 mg/kg, *i.p.*) normalized the expression of altered phosphorylated signaling molecules in the NAc of ENT1^{-/-} mice. Representative blots and expression levels are expressed as fold change compared to ENT1^{+/+} mice after normalization with GAPDH. Representation of phosphoprotein: pNg (Ser36) [$t(14) = 4.2, p < 0.001$], pPKC γ (Thr514), pCaMKII (Thr286), pCREB (Ser133). * $p < 0.05$ compared to ENT1^{+/+} mice after normalization by GAPDH by unpaired, two-tailed *t*-test. **(B)** Normalization of PP1/PP2A activity in ENT1^{-/-} mice after the treatment of CGP37849. $n = 8$ for each genotype. **(C)** Ethanol consumption (g/kg/day) is reduced in both genotypes with

CGP37849 treatment. **(D)** Ethanol preference (%) is also reduced in both genotypes with CGP37849 treatment compared to saline-treated control (S). $n = 16$ for each genotype. All data are presented as mean \pm SEM.

Table 1

Altered protein expression in signaling transduction of the nucleus accumbens detected by iTRAQ method.

Protein ID	Protein	Fold*	S.E.	p value**
P35722	<i>Ng</i>	2.24	0.55	< 0.001
P62204	<i>CaM</i>	1.75	0.47	0.010
P70296	<i>Pebp1</i>	1.60	0.30	0.014
P43006	<i>Eaat2</i>	0.66	0.12	0.003
P68181	<i>Prkacb</i>	0.64	0.13	0.010
Control				
P16858	<i>Gapdh</i>	1.04	0.07	0.626
Q7TMM9	<i>Tubb2a</i>	0.97	0.05	0.838

* Fold represents expression in ENT1^{-/-} mice compared to ENT1^{+/+} mice.** By unpaired two-tailed *t*-test.